

LETTER • OPEN ACCESS

Subhourly rainfall in a convection-permitting model

To cite this article: Edmund P Meredith *et al* 2020 *Environ. Res. Lett.* **15** 034031

View the [article online](#) for updates and enhancements.

Environmental Research Letters



LETTER

Subhourly rainfall in a convection-permitting model

OPEN ACCESS

RECEIVED
18 October 2019

REVISED
2 January 2020

ACCEPTED FOR PUBLICATION
3 January 2020

PUBLISHED
26 February 2020

Edmund P Meredith¹ , Uwe Ulbrich  and Henning W Rust 

Institut für Meteorologie, Freie Universität Berlin, Carl-Heinrich-Becker-Weg 6-10, D-12165, Berlin, Germany

¹ Author to whom any correspondence should be addressed.

E-mail: edmund.meredith@met.fu-berlin.de

Keywords: subhourly precipitation, convection-permitting model, climate, precipitation, high resolution

Supplementary material for this article is available [online](#)

Original content from this work may be used under the terms of the [Creative Commons Attribution 4.0 licence](#).

Any further distribution of this work must maintain attribution to the author(s) and the title of the work, journal citation and DOI.

**Abstract**

Convection-permitting models (CPMs)—the newest generation of high-resolution climate models—have been shown to greatly improve the representation of subdaily and hourly precipitation, in particular for extreme rainfall. Intense precipitation events, however, often occur on subhourly timescales. The distribution of subhourly precipitation, extreme or otherwise, during a rain event can furthermore have important knock-on effects on hydrological processes. Little is known about how well CPMs represent precipitation at the subhourly timescale, compared to the hourly. Here we perform multi-decadal CPM simulations centred over Catalonia and, comparing with a high temporal-resolution gauge network, find that the CPM simulates subhourly precipitation at least as well as hourly precipitation is simulated. While the CPM inherits a dry bias found in its parent model, across a range of diagnostics and aggregation times (5, 15, 30 and 60 min) we find no consistent evidence that the CPM precipitation bias worsens with shortening temporal aggregation. We furthermore show that the CPM excels in its representation of subhourly extremes, extending previous findings at the hourly timescale. Our findings support the use of CPMs for modelling subhourly rainfall and add confidence to CPM-based climate projections of future changes in subhourly precipitation, particularly for extremes.

1. Introduction

Short-duration, high-intensity precipitation events are a leading cause of flash flooding, posing health and economic risks to society. Realistic modelling of such events is thus important in both weather forecasting and climate projections. Such heavy precipitation events typically, though not always, result from atmospheric convection and are in Europe most common in summer or autumn, dependent on regional factors [1]. Realistic modelling of such extremes has in the past been hindered by inadequate spatial resolution in models, meaning that deep convective processes cannot be resolved and must instead be estimated via parametrization schemes [2], e.g. Such lower-resolution climate models produce subdaily extremes which are in general too spatially diffuse, too temporally persistent and with too-low local intensity maxima [3], as well as a diurnal convective cycle which peaks prematurely [4].

With increasing computational power, the use of ‘convection-permitting models’ (CPMs)—that is,

high-resolution atmospheric models (grid spacing <4 km) which can directly simulate deep-convective processes—has become more common in meteorology and climate science. This is driven by the added value of CPMs over lower-resolution models which require convective parametrization schemes [5]. The greatest added value of CPMs is found in their representation of precipitation [6], in particular subdaily convective extremes. At the hourly scale, CPMs greatly improve the representation of intense summertime precipitation events: in terms of their spatial patterns, intensities and temperature scaling [3, 7–13]. While CPMs have been shown to reduce the wet hour frequency bias [13], they may still overestimate the fractional contribution of intense events to total precipitation, with biases in the fractional contributions of light to moderate events seemingly regionally dependent [8]. CPMs also reduce the ‘drizzle problem’ found in coarser models [7], whereby light rainfall is too persistent, and tend to more realistically represent the frequency of short intense events [3, 8]. In addition

to a better representation of vertical mixing [14], the added value of CPMs may extend to future changes in precipitation extremes: CPMs have shown enhanced intensification of extremes in response to warming [15–17] and diurnal differences in future scaling [18] for certain regions.

At the subhourly temporal scale, there is a lack of CPM evaluation studies and less is known about how well CPMs simulate subhourly precipitation (extreme or non-extreme), primarily due to a lack of appropriate observations. Subhourly precipitation, however, can play a crucial role in incidents of flash-flooding. Hydrological models also benefit greatly from high spatiotemporal resolution input [19] for stress testing of hydraulic infrastructure, process-orientated case studies [20] and future climate-change ‘storylines’ [21]. While there have been tentative studies looking at future changes in extreme subhourly precipitation [22, 23], without evaluation of CPM subhourly precipitation for the present climate we cannot have confidence in the future projections. Evaluation of modelled subhourly rainfall has thus been identified as a key effort in climate modelling [22]. The improved performance of CPMs in representing hourly extremes need not necessarily translate to the subhourly scale. It could be, for example, that events of subhourly duration are too weak and too long-lasting in models, or too intense and too short-lived, giving accurate hourly totals for the wrong reasons and misrepresenting subhourly totals. The same amount of precipitation spread over different time periods will affect many land surface processes [19], such as the amount of precipitation absorbed by the soil, converted to runoff, and re-evaporated by the atmosphere, all of which are important considerations in hydrological modelling and climate modelling in general. Future changes in the intermittency of rainfall may be masked at hourly timescales, leading to flawed estimates of changes in precipitation intensities and their impacts [24]. Identifying shortcomings in the character of modelled subhourly precipitation is thus important for ongoing CPM development. To assess the realism of subhourly rainfall in a CPM, we make use of a high temporal-resolution rain-gauge network from the city of Barcelona, Spain. The precipitation climatology of our study region is characterised by relatively benign conditions in winter and spring, with the risk of intense rainfall increasing as the Mediterranean Sea warms, and peaking during August, September and October (ASO; figure 1(a)) [25]. Intense ASO rainfall here is typically associated with either (i) localised thermal convection, or (ii) low pressure systems over the north-western Mediterranean advecting warm moist air, often with embedded convection, towards north-eastern Spain [26]. Ocean-atmosphere heat and moisture exchange is a dominant factor in event intensities [26, 27] and intense events can be either of synoptic- or meso-scale origin. Focusing our analyses on ASO thus encapsulates the months with

the most intense events, as well as extremes of large- and local-scale origin.

2. Methods

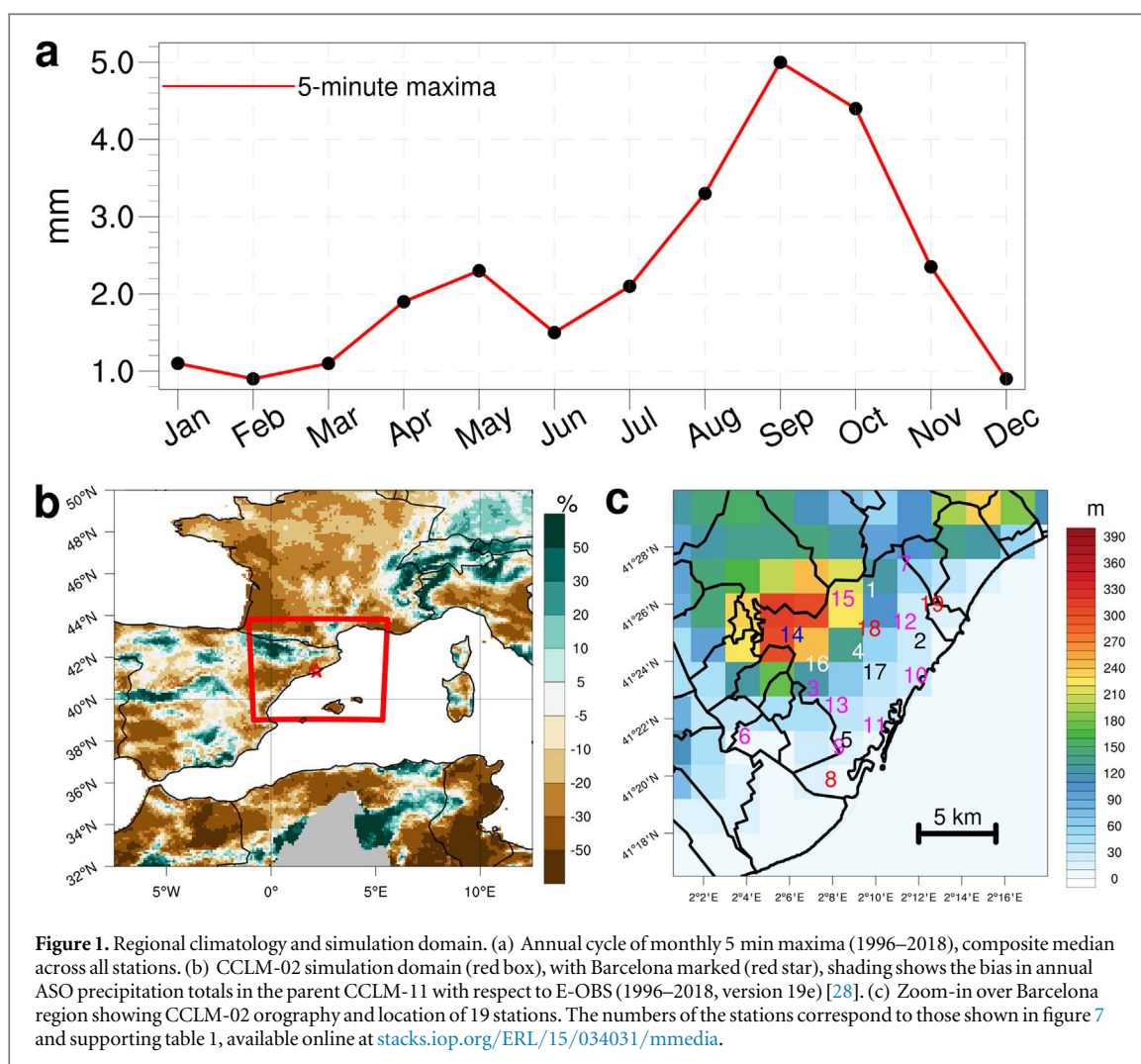
2.1. Observational data

We utilise a network of rain gauges from the greater Barcelona region [29–32], e.g. The network consists of 0.1 mm tipping bucket rain gauges; the brand is Geónica SA and gauges have a 400 cm² collector funnel. The homogeneity of the series has been verified in Lana *et al* (2019) [30] via the Wald-Wolfowitz run test of randomness and the Mann-Kendall trend test. From this network we select 19 gauges (figure 1(c), supporting table 1) with continuous measurements between 1.8.1996 and 31.10.2018, giving 23 years of ASO data with on average 2.6% missing values. For 3 of the 19 stations, coverage ends with ASO 2015, 2016 and 2017, respectively. 5, 15, 30 and 60 min totals are derived for each station. Tipping bucket gauges are subject to errors associated with splashing, evaporation and wind; such systematic errors are largest for low rain rates and at temporal aggregations less than 10 minutes, becoming negligible above 15 min time-scales [33, 34]. For the temperature scaling of daily precipitation maxima presented in figure 8, we use daily mean temperatures from the 0.11° Spain02 data set [35].

2.2. Model and simulations

Convection-permitting simulations at 0.02° resolution are performed with version 5.00_clm9 of the COSMO regional model in climate mode (CCLM) [36]. CCLM is the community model of the German regional climate research community jointly further developed by the CLM-Community (<https://clm-community.eu/>). The simulation domain is centred on Barcelona (figure 1(b)) and has horizontal dimensions of 241 × 241 grid cells and 60 unevenly spaced terrain-following vertical levels, with the lowest model level at 20 m and a model top at 22 km. The high resolution of the 0.02° CCLM (CCLM-02) allows parametrization of deep convection to be switched off, while shallow convection is parametrized based on the Tiedtke scheme [2]. The model time step is 20 s and the microphysics scheme which produces grid-scale precipitation is called at every time step.

We perform four-month time slice simulations from July 1st to October 31st each year from 1996 to 2018. Initial and boundary conditions come from 0.11° CCLM (CCLM-11) simulations over the EURO-CORDEX domain nested in ERA-Interim reanalysis [37]; these forcing data exhibit a dry bias of about –30% in our study region (figure 1(b)). Years 1996–2008 of the CCLM-11 runs were simulated continuously by the CLM-Community [38] as part of EURO-CORDEX [39], while years 2009–2018 were simulated by the present authors [20, 40]. Neither



CCLM-11 nor CCLM-02 use nudging. From the CCLM-02 simulations, the month of July is discarded for soil-moisture spinup, leaving ASO as the analysis months; soil moisture is of lower-order importance, compared to the maritime influence, for ASO precipitation in Barcelona. Precipitation totals are saved at 5 min intervals.

For comparison with observations, CCLM-02 5 min precipitation data are interpolated to the station coordinates using the nearest-neighbour method and rounded to 0.1 mm precision, before totals for longer aggregation times are summed. While a synchronous reproduction of observed day-to-day variability at each station is not expected from the regional model, individual locations should be climatologically representative [41], all the more so with our CPM domain not being too far from the CCLM-11 inflow boundary.

2.3. Analyses

Analyses are focused on accumulation periods of 5, 15, 30 and 60 min and begin by considering modelled biases in standard diagnostics (figures 2, 3). Here intensity diagnostics are computed for ‘wet periods’, where a ‘wet period’ is an accumulation period with at least 0.1 mm of precipitation (the record precision in

the observations); return levels (figure 2) are estimated by fitting a generalized extreme value distribution [42] to annual ASO maxima using the ‘isnev’ [43] R-package. We then look in more detail at biases across the entire precipitation spectrum (figure 4) using the ‘Analysing Scales of Precipitation (ASoP)’ method of Klingaman *et al* (2017) [44]; see also Berthou *et al* (2018) [8] for further elucidation. The focus then shifts to the temporal characteristics of modelled precipitation (figures 5, 6), by looking at combined wet-spell and intensity biases, as well as biases in event ‘wet time fraction’ (WTF) [45], where the ‘wet time fraction’ is the fraction of 5 min intervals within an accumulation period in which precipitation occurs. The spatial realism of modelled precipitation is then considered by comparing the conditional probabilities of wet-event thresholds being exceeded between stations (figure 7); this type of analysis is sometimes called ‘Event Coincidence Analysis’ [46]. The statistical significance with respect to interannual variability of the biases presented in figures 4–7 is estimated via bootstrap resampling of ASO blocks with replacement, similar to [3, 15, 47]. We conclude by considering the scaling of extreme precipitation with temperature [48], e.g. in observations and CCLM-02

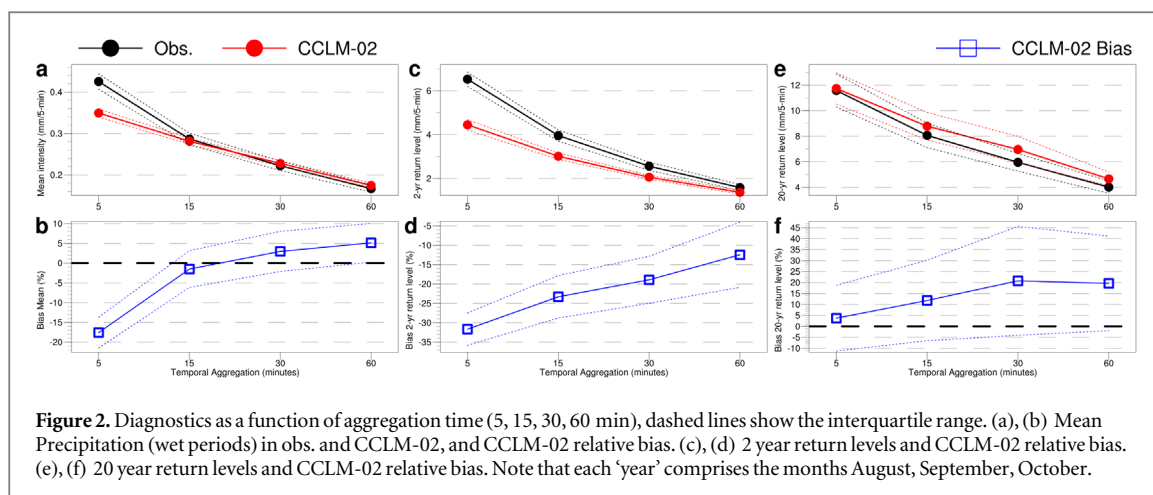


Figure 2. Diagnostics as a function of aggregation time (5, 15, 30, 60 min), dashed lines show the interquartile range. (a), (b) Mean Precipitation (wet periods) in obs. and CCLM-02, and CCLM-02 relative bias. (c), (d) 2 year return levels and CCLM-02 relative bias. (e), (f) 20 year return levels and CCLM-02 relative bias. Note that each ‘year’ comprises the months August, September, October.

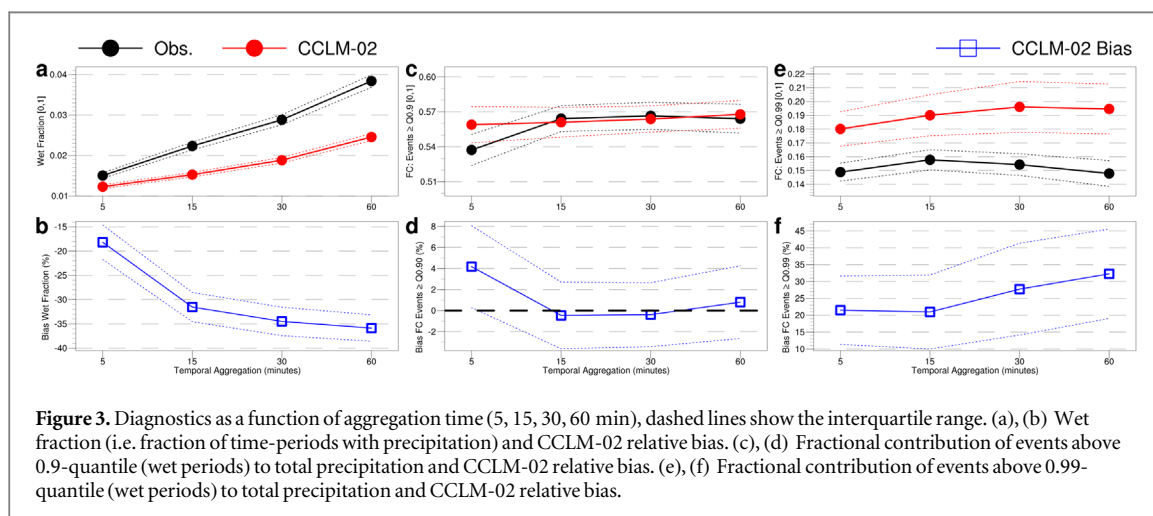


Figure 3. Diagnostics as a function of aggregation time (5, 15, 30, 60 min), dashed lines show the interquartile range. (a), (b) Wet fraction (i.e. fraction of time-periods with precipitation) and CCLM-02 relative bias. (c), (d) Fractional contribution of events above 0.9-quantile (wet periods) to total precipitation and CCLM-02 relative bias. (e), (f) Fractional contribution of events above 0.99-quantile (wet periods) to total precipitation and CCLM-02 relative bias.

(figure 8; further details in figure caption); analysis here is restricted to the years 1996–2015 due to the length of the Spain02 data set [35]. Note that all biases presented are computed by calculating the individual biases for each station and taking the mean of these biases, as opposed to pooling all stations together and computing biases based on diagnostics of the pooled data.

3. Results and discussion

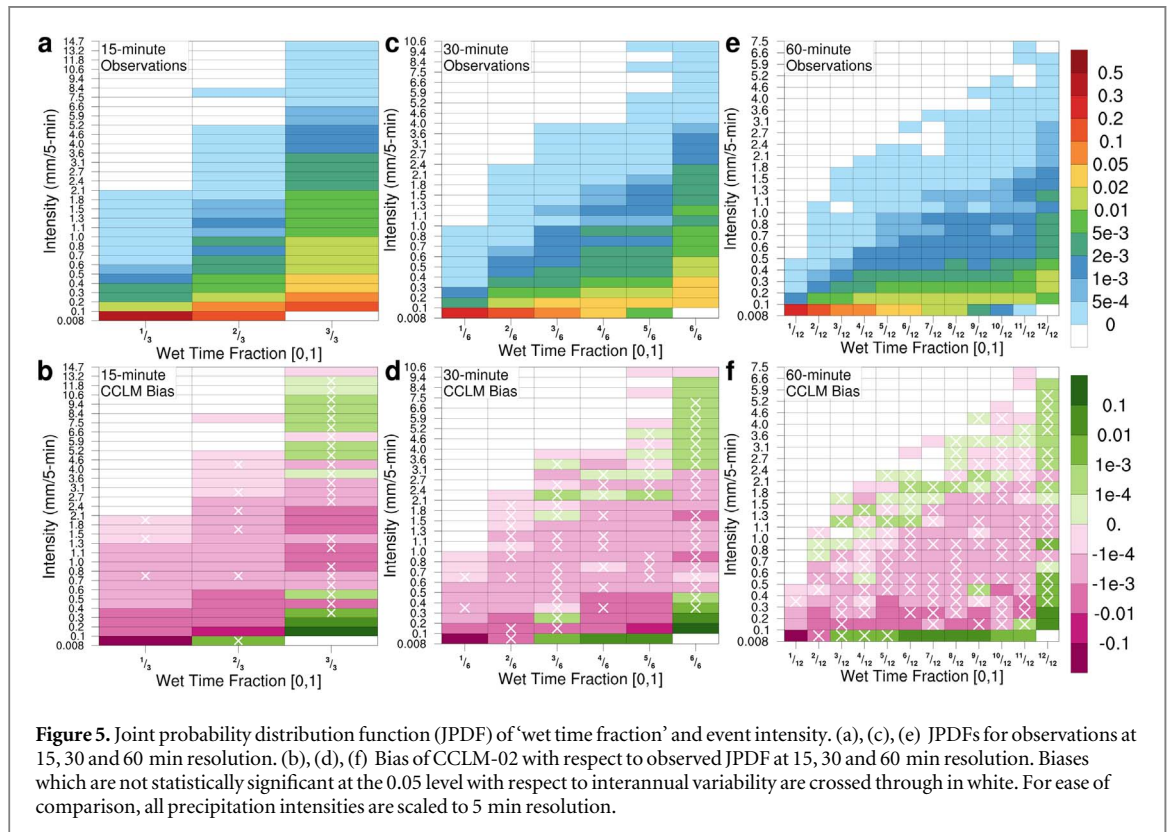
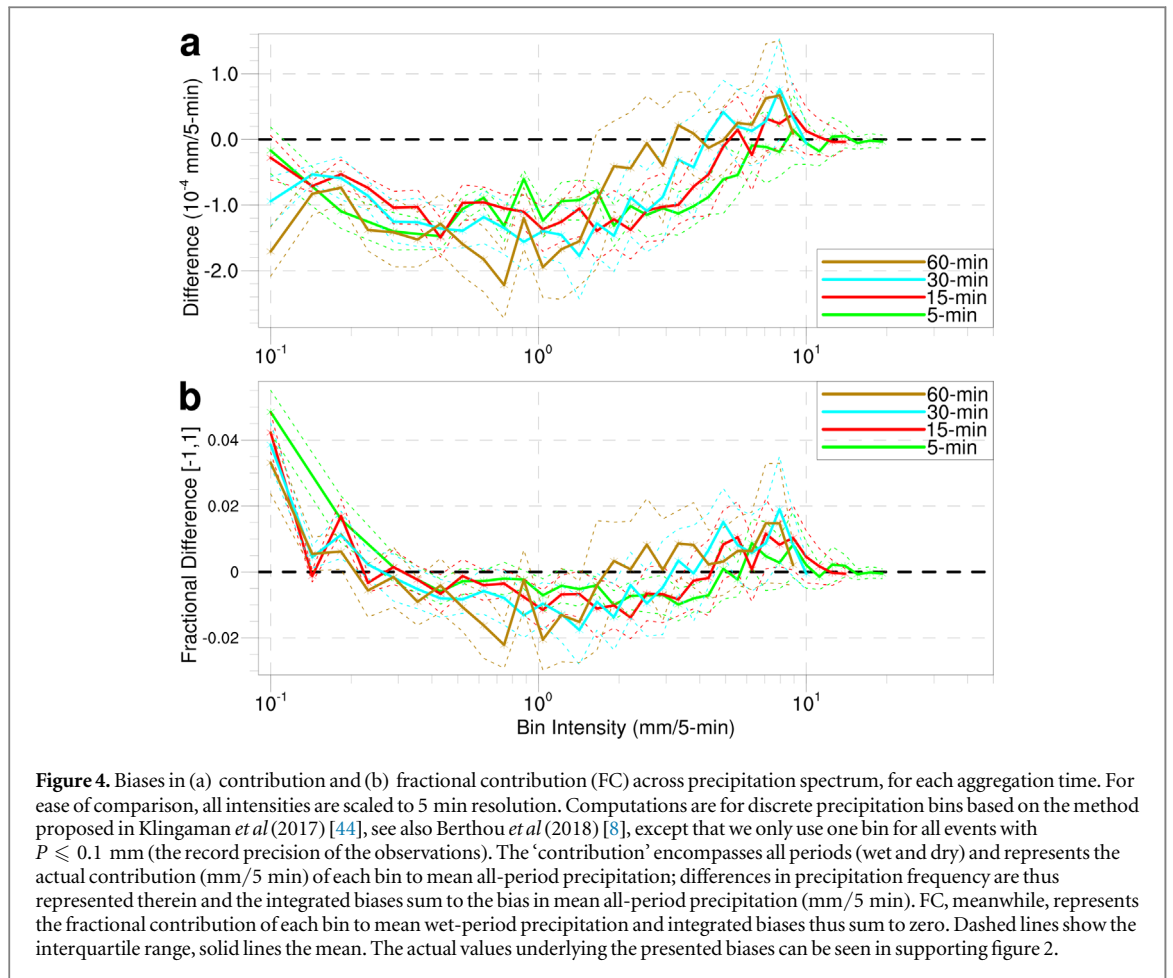
In the following sub-sections we present our results with an emphasis on differences in model performance at different aggregation times (5, 15, 30 and 60 min).

3.1. Climatology and standard diagnostics

CCLM-02 displays a bias of -18% in the mean intensities of 5 min wet-events, which decreases to the $\pm 5\%$ range at 15 and 30 min aggregations, slightly less than at hourly aggregation (figures 2(a), (b)). For stronger (2 year (ASO) return level) events, a clear negative intensity bias in CCLM-02 appears, which decreases with increasing aggregation time (figures 2(c), (d)). For 20 year (ASO) return levels, subhourly model

performance improves, with the negative intensity bias eliminated and a 5 min bias of $<5\%$ (figures 2(e), (f)). The mean-strong-intense diagnostics all paint a picture of model biases in event intensity trending positively with increasing aggregation time.

While simple event-intensity diagnostics suggest somewhat degraded model performance for mean and 2 year return level events (figures 2(a)–(d)) as aggregation times shorten, the constraint of total ASO precipitation—which is independent of aggregation time—implies that the opposite is true for the occurrence frequency of wet events (figures 3(a), (b)). The wet fraction is negatively biased for all aggregation times (indicating too infrequent precipitation), with biases increasing from -15% at 5 min to over -30% at aggregations ≥ 15 min. The combination of too infrequent precipitation and mean precipitation being either too weak or similar to observations largely explains the dry bias in summed ASO precipitation totals which CCLM-02 produces (roughly -30% , not shown). The influence of the dry bias in the forcing model (figure 1(b)) must here be kept in mind. A similar, though less decisive, reversal in the bias-aggregation trends from figure 2 is found for the fraction of total precipitation accounted for by events above the wet 0.9- and 0.99-quantiles (figures 3(c)–(f)). For the



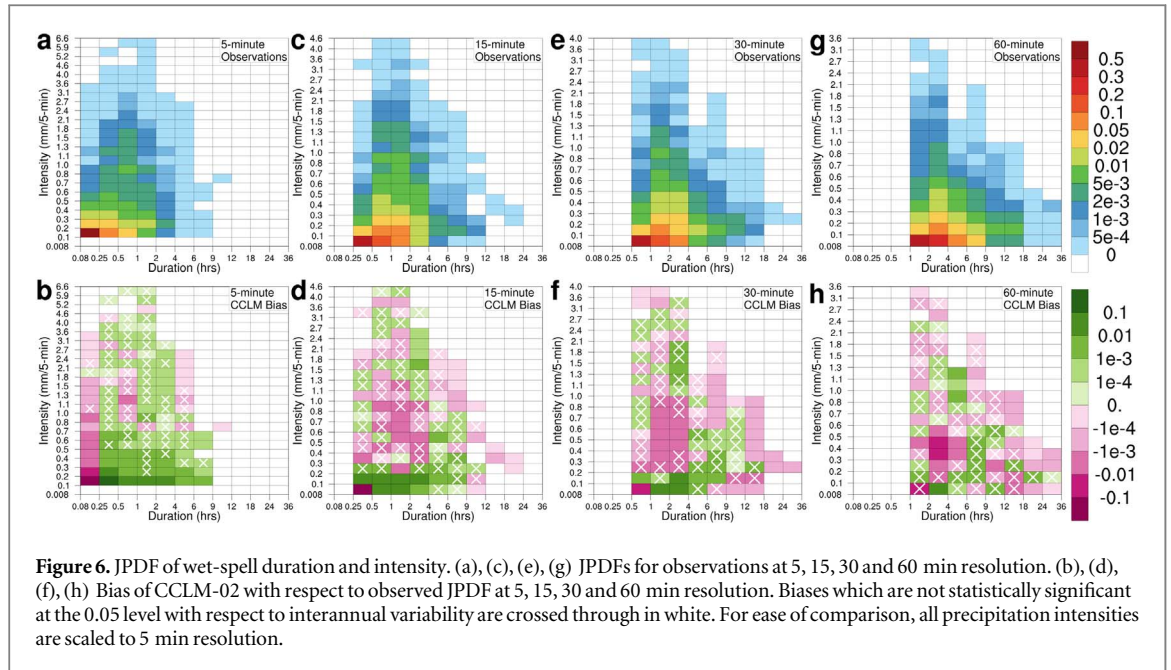


Figure 6. JPDF of wet-spell duration and intensity. (a), (c), (e), (g) JPDFs for observations at 5, 15, 30 and 60 min resolution. (b), (d), (f), (h) Bias of CCLM-02 with respect to observed JPDF at 5, 15, 30 and 60 min resolution. Biases which are not statistically significant at the 0.05 level with respect to interannual variability are crossed through in white. For ease of comparison, all precipitation intensities are scaled to 5 min resolution.

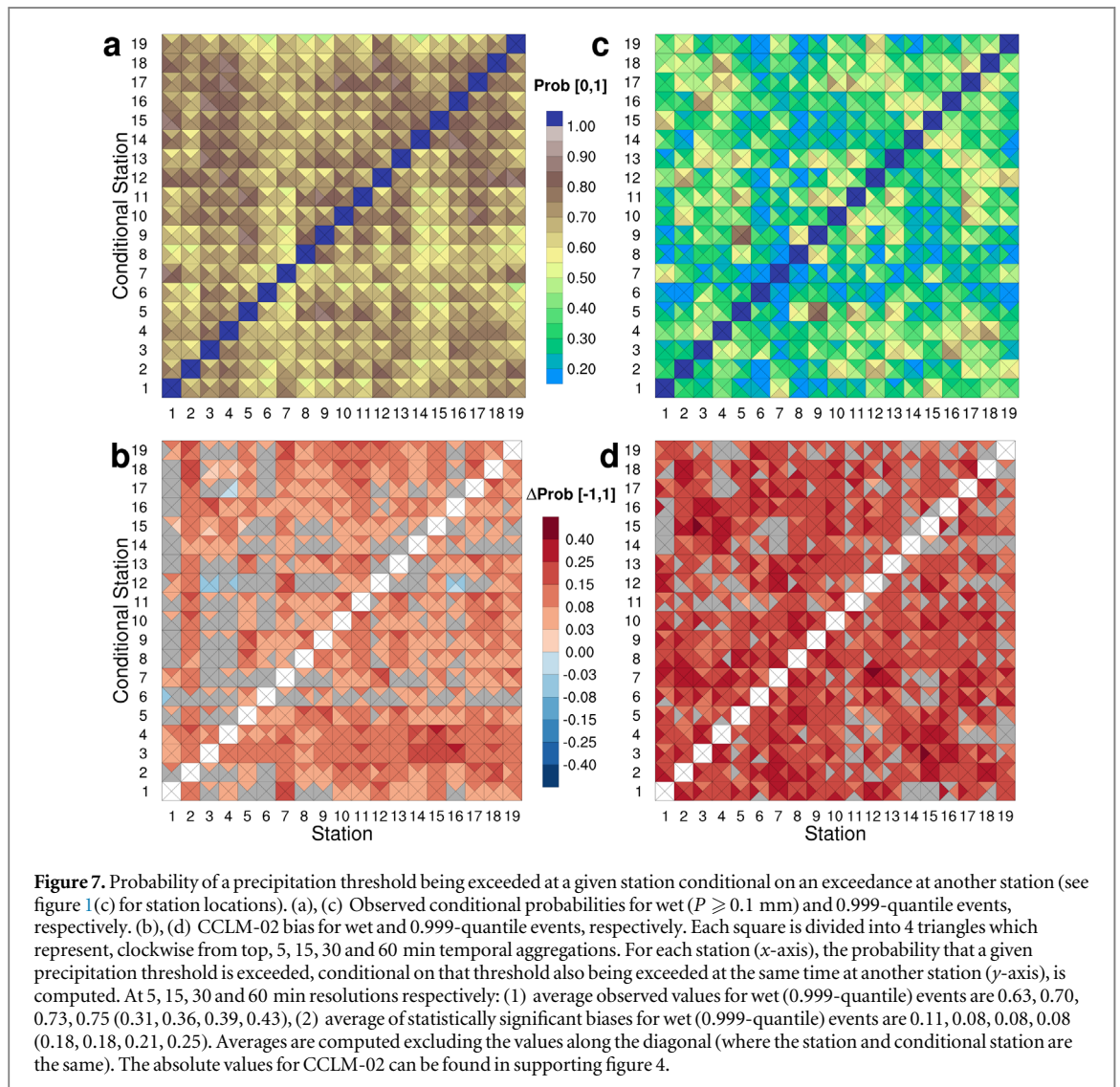


Figure 7. Probability of a precipitation threshold being exceeded at a given station conditional on an exceedance at another station (see figure 1(c) for station locations). (a), (c) Observed conditional probabilities for wet ($P \geq 0.1$ mm) and 0.999-quantile events, respectively. (b), (d) CCLM-02 bias for wet and 0.999-quantile events, respectively. Each square is divided into 4 triangles which represent, clockwise from top, 5, 15, 30 and 60 min temporal aggregations. For each station (x -axis), the probability that a given precipitation threshold is exceeded, conditional on that threshold also being exceeded at the same time at another station (y -axis), is computed. At 5, 15, 30 and 60 min resolutions respectively: (1) average observed values for wet (0.999-quantile) events are 0.63, 0.70, 0.73, 0.75 (0.31, 0.36, 0.39, 0.43), (2) average of statistically significant biases for wet (0.999-quantile) events are 0.11, 0.08, 0.08, 0.08 (0.18, 0.18, 0.21, 0.25). Averages are computed excluding the values along the diagonal (where the station and conditional station are the same). The absolute values for CCLM-02 can be found in supporting figure 4.

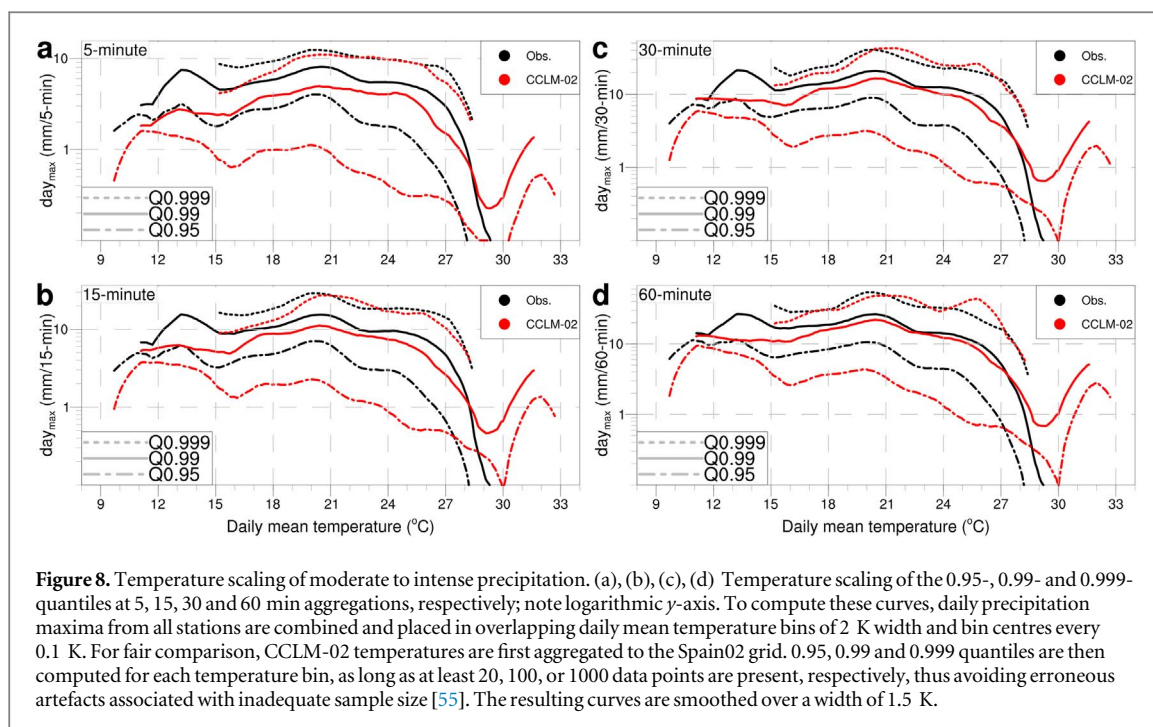


Figure 8. Temperature scaling of moderate to intense precipitation. (a), (b), (c), (d) Temperature scaling of the 0.95-, 0.99- and 0.999-quantiles at 5, 15, 30 and 60 min aggregations, respectively; note logarithmic y -axis. To compute these curves, daily precipitation maxima from all stations are combined and placed in overlapping daily mean temperature bins of 2 K width and bin centres every 0.1 K. For fair comparison, CCLM-02 temperatures are first aggregated to the Spain02 grid. 0.95, 0.99 and 0.999 quantiles are then computed for each temperature bin, as long as at least 20, 100, or 1000 data points are present, respectively, thus avoiding erroneous artefacts associated with inadequate sample size [55]. The resulting curves are smoothed over a width of 1.5 K.

former, model biases are below $\pm 5\%$. For events above the 0.99-quantile, a bias of at least 20% in their contribution to total precipitation is found, hinting that overly-heavy intense events (figures 3(e), (f)) may be partly mitigating negative biases at lesser intensities (figures 2(a)–(d)).

3.2. Observed and modelled distributions

To look in more detail at the contributors to the mean model bias, we consider differences in the contribution and fractional contribution (FC) of bins of discrete precipitation intensity to mean precipitation (figure 4), following the ASoP method of Klingaman *et al* (2017) [44]; see figure 4 caption and Berthou *et al* (2018) [8] for further explanation. The contribution to mean precipitation of intensities from 0.2 to 2 mm/5 min shows a clear dry bias across all aggregation times (figure 4(a)); this negative bias for the bulk is also found in the FCs (figure 4(b)). While light and drizzle-like events ($P \leq 0.1$ mm/5 min) also show a negative bias in their contribution to mean precipitation, their FC is positively biased. Taken together, this could suggest that in CCLM-02 light events are too persistent or that moderate ($0.2 \leq P \leq 2$ mm/5 min) events are too short-lived. An often cited advantage of CPMs is that they ameliorate the ‘drizzle problem’ [49, 50], e.g.—i.e. excessive persistent light rain—found in coarser models with convective parametrizations [3, 7], making the former less likely. Additionally, at the 60 min timescale CCLM-02 shows a mostly reduced contribution bias for event intensities below 2 mm/60 min compared to its parent CCLM-11 (supporting figure 1(a)); verification at subhourly aggregations is not possible due to an absence of subhourly CCLM-11 data. CPMs with parametrized shallow convection, as

here in CCLM-02 [2], often produce precipitation which is more persistent in character than those without [8]. Additional experiments, however, suggest that the shallow convection scheme is not the source of the positive FC bias for light precipitation (supporting figure 3 and accompanying discussion), but rather that the FC bias results from an insufficient contribution of event intensities between 0.2 and 2 mm/5 min to mean precipitation, as speculated above and further supported by the negative wet fraction bias (figures 3(a), (b)). Also worth noting is that the CCLM-02 FC biases for event intensities below 9 mm/hour are generally less than those in CCLM-11 (supporting figure 1(b)).

For intensities above 3 mm/5 min, CCLM-02 performs much better. It is only at intensities above 5 mm/5 min that for all aggregation times CCLM-02 shows contribution and FC biases whose interquartile ranges include zero. When interpreting the biases for all intensities, the dry bias in the parent CCLM-11 (figure 1(b)) should be kept in mind. Furthermore, caution should be exercised when interpreting the light precipitation $O(0.1$ mm/5 min) biases, because at these intensities the record precision of the gauge (0.1 mm), and hence uncertainty, is large relative to the precipitation totals and systematic gauge errors are also highest [33]. The key finding is, however, independent of the magnitude of the biases: for a given set of lateral boundary conditions (CCLM-11), the CCLM-02 precipitation bias does not worsen with shortening temporal aggregation.

3.3. Event intensities and temporal characteristics

The high temporal resolution data allow us to consider the ‘wet time fraction’ [45], i.e. the fraction of 5 min

intervals within an aggregation period in which precipitation is registered ($P \geq 0.1$ mm), which can give insight into the intermittence and persistence of observed and modelled precipitation. Considering the joint probability distribution function (JPDF) of WTF and intensity, observations indicate that the most frequent class of wet-event is short-lived light precipitation with the minimum possible WTF (i.e. one 5 min interval) within its accumulation period (figures 5(a), (c), (e)). This class of wet-event is systematically underrepresented amongst CCLM-02 wet periods—across all aggregation times (figures 5(b), (d), (f)). Instead, precipitation intensities of 0.1 mm/5 min or lower which persist across a higher fraction of the accumulation period are too prevalent. This overrepresentation is also evident in slightly stronger events ($P < 0.3$ mm/5 min), which are much more likely to feature continuous precipitation ($\text{WTF} = 1$) in CCLM-02 than in observations. As intensities increase above 0.3 mm/5 min, WTF biases are either reduced or insignificant, perhaps because such events, by their nature, tend to have longer lifespans.

To learn more about the persistence and intermittency of modelled precipitation, we consider the JPDF of wet-spell duration and intensity, where a wet-spell is defined as one or more successive aggregation periods in which precipitation is registered. Observations suggest that the most common class of wet-spell is a single accumulation period with $P \leq 0.1$ mm when scaled to 5 min resolution (figures 6(a), (c), (e), (g)). Multi-hour wet-spells with $P \leq 0.1$ mm/5 min or single-period wet-spells with $P \geq 2$ mm/5 min are the most rare. As might be expected from the WTF results, wet-spells of single-aggregation-period duration and low intensity ($P \leq 0.1$ mm/5 min) are underrepresented amongst CCLM-02 wet-spells (figures 6(b), (d), (f), (h)). The wet-spell duration and intensity JPDF additionally shows that this persistence of light precipitation in CCLM-02 extends beyond single aggregation periods and results in multi-hour low-intensity ($P \leq 0.2$ mm/5 min) wet-spells having increased probability, particularly for subhourly aggregation times. Wet-spells of moderate intensity ($0.2 < P \leq 1.0$ mm/5 min) are, on the other hand, generally too infrequent at 15, 30 and 60 min aggregations, supporting the conclusion from section 3.2 that such events are too short-lived in CCLM-02. At 5 min aggregation, however, significant negative frequency biases for intensities below 1 mm/5 min are restricted to single-period (5 min) wet-spells. For the least common intensity-duration combinations the model biases are lower and often non-significant, painting a less clear picture, though echoing the better performance for extremes shown in figure 4. Overall, and considering equivalent wet-spell durations, there is no clear sign that shorter aggregation times increase biases. It is worth noting that for both JPDF analyses, the strongest biases at each aggregation are found for the shortest WTF/duration and lowest intensity, precisely the

conditions under which tipping bucket errors are largest [33, 34] and, hence, uncertainty highest.

3.4. Spatial realism

One potential contributory factor to biases in precipitation statistics is that the simulated precipitation features may be too spatially diffuse (localized), resulting in the larger (smaller) precipitating cloud spending extended (reduced) time over a given location and hence precipitation falling over a longer (shorter) period. The spatial coherence of observed precipitation is typically lowest for extremes and shorter aggregation times, and highest for large-scale events (which tend to be less intense) and longer aggregation times. This is confirmed (figures 7(a), (b)) for the Barcelona gauge network [31]. For 0.999-quantile events, only adjacent gauges show coincident probability scores over 0.6 (e.g. gauges 5/9, 3/16, 4/17/18), whereas such high scores are ubiquitous for wet-threshold ($P \geq 0.1$ mm) events. Unsurprisingly, gauges which occupy the same CCLM-02 grid cell (gauges 5/9 and 3/16, see figure 1(c)) still show scores well below unity, highlighting the issue of location representativeness in models [41] (supporting figure 4). For CCLM-02, analyses indicate that single precipitation events tend to cover too large an area. For the simple wet-event threshold, the probability of a wet event occurring at a given station location, conditional on a wet event at another station, is almost uniformly higher in CCLM-02 than found in observations, for all aggregation times (figure 7(c)). This could be partly because less intense ($P \leq 0.3$ mm/5 min) events—which are by nature typically diffuse—constitute a higher fraction of total events in CCLM-02 than in observations (section 3.2, figure 4(b)). This positive bias, indicating modelled events which cover too large an area, however also exists for 0.999-quantile events (figure 7(d)), telling us that even in the high-resolution CCLM-02, precipitation events of all intensities cover too large an area. This is perhaps not surprising when considering that the precipitation produced in the model represents grid cell averages, in our case over a grid cell of nearly 5 km², which has the effect of smoothing-out subgrid-scale events over a larger area [51]. Crucially, there is no evidence of the bias worsening at shorter aggregations.

3.5. Temperature scaling of moderate to extreme events

Analyses thus far suggest that the CCLM-02 subhourly performance is best for extremes, consistent with the main added value of CPMs [5]. We therefore conclude our study by assessing the temperature scaling of extreme precipitation—often referred to as ‘binning scaling’ [52]. Theory suggests that precipitation extremes should scale positively with increasing temperature until moisture availability becomes limited, at which point a negative scaling emerges [53]. The

CCLM-02 temperature-scaling curves (figure 8; see caption for details) show closer agreement with observations for higher quantiles. For the highest (0.999) quantile, the agreement on extreme precipitation temperature scaling is excellent for all aggregation times. Above 15 °C, the form of the observed and model-simulated extreme scaling curves (0.99, 0.999-quantile) additionally closely matches that found in Drobinski *et al* (2018) [54] for extreme subhourly precipitation at a station south-west of Barcelona: intensification with increasing temperature, before a levelling-off between 20 and 25 °C, followed by a downturn in precipitation intensity with further temperature increase. Previous work [45] suggested that such downturns in intensity at higher temperatures are not a feature of subhourly precipitation extremes, which can instead keep intensifying. For our study region the observations disagree and CCLM-02 well replicates the observed scaling at all temporal aggregations. Interestingly, CCLM-02 also shows an uptick in precipitation at very high daily mean temperatures, which is not found in observations.

4. Further discussion and conclusions

Extensive work evaluating hourly precipitation in CPMs [3, 7–10, 12, 13] has enabled a growing number of CPM studies of future hourly precipitation [18, 56–58] and given confidence in the resulting projections. To date, this has not been the case with subhourly CPM precipitation. Our work firstly confirms previous findings [6–9, 13] at the hourly scale: despite remaining biases, CCLM-02 reduces the precipitation bias across almost all intensity ranges (supporting figure 1). While we cannot compare subhourly CCLM-02 precipitation with that from the coarser parent CCLM-11 (due to a lack of subhourly CCLM-11 data), our findings broadly indicate that biases in subhourly precipitation in CCLM-02 are no worse than those found at the hourly scale. This result should add confidence to future projections of subhourly precipitation based on CPMs.

The forcing data (CCLM-11) for our study region are dry-biased and this is reflected in an overall dry bias in CCLM-02, most prominently characterized by an insufficient contribution to mean precipitation from moderate-intensity events, which in turn leads to light events having too high a fractional contribution (Figure 4) and low-intensity persistent wet-spells being overrepresented amongst all wet-spells (figure 6), irrespective of the aggregation time. Additional tests without parametrized shallow convection did not improve on these biases, despite reducing the total amount of light precipitation. The reliability of the observations must also be borne in mind: the strongest model biases are often found for low intensities and short durations/WTFs (figures 4–6), exactly the conditions under which tipping bucket gauges

suffer most from systematic errors [33, 34]. Such results therefore come with higher uncertainty and should be treated with caution.

Between different diagnostics, our results occasionally give mixed signals as to the best-modelled aggregation time. For example, while the 2 year return level bias decreases with increasing aggregation time, the wet fraction bias increases with increasing aggregation time (figures 2, 3). On the whole, however, there is no conclusive evidence for a deterioration in model performance at the subhourly aggregation times investigated. For the contributions and fractional contributions of different intensities to mean precipitation (figure 4), biases for all aggregation times are low and same-signed for moderate to intense events; subhourly precipitations are at least as accurate as their hourly counterpart. For the spatial representation of precipitation events, even at 0.02° resolution CCLM produces events which are too spatially diffuse, however this bias is again consistent across aggregation times (figure 7).

Turning to precipitation extremes, the so far clearest source of added value identified in CPMs at the subdaily scale [6, 7, 9], the performance of CCLM-02 at subhourly aggregations can be considered very good. We have shown that CCLM-02 not only reliably simulates extremes at hourly resolution, but also across all subhourly aggregation times tested. The lowest biases in the contribution and fractional contribution to mean precipitation are for intense to extreme events over 5 mm/5 min, across all aggregation times, with biases smallest for the shortest aggregation times (figure 4). Biases in intensity-WTF and intensity-wet-spell JPDFs are also lowest for extremes and are of similar magnitude across aggregation times (figures 5, 6). The temperature scaling of extreme precipitation in CCLM-02 is highly realistic across all aggregation times and well captures the observed downturn at higher temperatures (figure 8).

Our study suggests that CPM users need not fear a degradation in precipitation projections or forecasts when moving from hourly to subhourly resolutions. While biases still exist, we find no compelling evidence that subhourly biases are any worse than those at the hourly scale. This is emphatically the case for extremes, the class of event for which higher spatio-temporal resolutions are of most interest. We conclude by re-stating the utility of CPMs as a tool for studying extreme precipitation, associated mechanisms and changes therein at the hourly scale [16, 18], and by extending this endorsement to extreme precipitation at subhourly timescales.

Acknowledgments

This study was funded by the European Commission through the H2020 project BINGO (<http://projectbingo.eu/>), grant agreement 641739. EM

additionally received part funding from the EUREX project of the Helmholtz Association (HRJRG-308). We thank Barcelona Cicle de l'Aigua SA (BCASA), Adjuntament de Barcelona and Blanca Aznar for providing the observational data. We further thank Maria Carmen Llasat for assistance with the observations and providing valuable guidance, and Beniamino Russo. We also thank M Göber and F Fundel for helpful discussions. Computing resources were provided by the German Climate Computing Centre (DKRZ), the North-German Supercomputing Alliance (HLRN), and ZEDAT of the Freie Universität Berlin. We thank the CLM-Community (<https://clm-community.eu/>) for producing part of the CCLM-11 simulations used as boundary forcing for CCLM-02 and for developing and maintaining the CCLM. We thank the producers of the Spain02 [35] and E-OBS [28] data sets. Analyses were performed with NCL [59] and R [60].

Data availability statement

The CCLM-02 simulations which support the findings of this study have been archived at the DKRZ World Data Center for Climate (<https://dkrz.de/up/systems/wdcc>) and are openly available at https://cera-www.dkrz.de/WDCC/ui/ceraresearch/entry?acronym=DKRZ_LTA_961_ds00007; the data set is citable as Meredith *et al* (2019) [61]. Observational data are available for non-commercial purposes from BCASA (<http://bcasa.cat/>).

ORCID iDs

Edmund P Meredith  <https://orcid.org/0000-0001-7555-0005>

Uwe Ulbrich  <https://orcid.org/0000-0001-7558-6622>

Henning W Rust  <https://orcid.org/0000-0003-0763-3954>

References

- Gaume E *et al* 2009 A compilation of data on European flash floods *J. Hydrol.* **367** 70–8
- Tiedtke M 1989 A comprehensive mass flux scheme for cumulus parameterization in large-scale models *Mon. Weather Rev.* **117** 1779–800
- Kendon E J, Roberts N M, Senior C A and Roberts M J 2012 Realism of rainfall in a very high-resolution regional climate model *J. Clim.* **25** 5791–806
- Hohenegger C, Brockhaus P and Schär C 2008 Towards climate simulations at cloud-resolving scales *Meteorol. Z.* **17** 383–94
- Prein A F *et al* 2015 A review on regional convection-permitting climate modeling: demonstrations, prospects, and challenges *Rev. Geophys.* **53** 323–61
- Brisson E, Van Weverberg K, Demuzere M, Devis A, Saeed S, Stengel M and van Lipzig N P M 2016 How well can a convection-permitting climate model reproduce decadal statistics of precipitation, temperature and cloud characteristics? *Clim. Dynam.* **47** 3043–61
- Fosser G, Khodayar S and Berg P 2015 Benefit of convection permitting climate model simulations in the representation of convective precipitation *Clim. Dynam.* **44** 45–60
- Berthou S, Kendon E J, Chan S C, Ban N, Leutwyler D, Schär C and Fosser G 2018 Pan-European climate at convection-permitting scale: a model intercomparison study *Clim. Dyn.* (<https://doi.org/10.1007/s00382-018-4114-6>)
- Ban N, Schmidli J and Schär C 2014 Evaluation of the convection-resolving regional climate modeling approach in decade-long simulations *J. Geophys. Res.-Atmos.* **119** 7889–907
- Chan S C, Kendon E J, Fowler H J, Blenkinsop S, Roberts N M and Ferro C A T 2014 The value of high-resolution met office regional climate models in the simulation of multihourly precipitation extremes *J. Clim.* **27** 6155–74
- Chan S C, Kendon E J, Roberts N M, Fowler H J and Blenkinsop S 2016 Downturn in scaling of UK extreme rainfall with temperature for future hottest days *Nat. Geosci.* **9** 24
- Zittis G, Bruggeman A, Camera C, Hadjinicolaou P and Lelieveld J 2017 The added value of convection permitting simulations of extreme precipitation events over the eastern Mediterranean *Atmos. Res.* **191** 20–33
- Ban N, Rajczak J, Schmidli J and Schär C 2018 Analysis of Alpine precipitation extremes using generalized extreme value theory in convection-resolving climate simulations *Clim. Dyn.* (<https://doi.org/10.1007/s00382-018-4339-4>)
- Hentgen L, Ban N, Kröner N, Leutwyler D and Schär C 2019 Clouds in convection-resolving climate simulations over Europe *J. Geophys. Res.: Atmos.* **124** 3849–70
- Kendon E J, Roberts N M, Fowler H J, Roberts M J, Chan S C and Senior C A 2014 Heavier summer downpours with climate change revealed by weather forecast resolution model *Nat. Clim. Change* **4** 570–6
- Meredith E P, Maraun D, Semenov V A and Park W 2015 Evidence for added value of convection-permitting models for studying changes in extreme precipitation *J. Geophys. Res.—Atmos.* **120** 12500–13
- Kendon E J, Ban N, Roberts N M, Fowler H J, Roberts M J, Chan S C, Evans J P, Fosser G and Wilkinson J M 2017 Do convection-permitting regional climate models improve projections of future precipitation change? *Bull. Am. Meteorol. Soc.* **98** 79–93
- Meredith E P, Ulbrich U and Rust H W 2019 The diurnal nature of future extreme precipitation intensification *Geophys. Res. Lett.* **46** 7680–9
- Dunkerley D L 2019 Rainfall intensity bursts and the erosion of soils: an analysis highlighting the need for high temporal resolution rainfall data for research under current and future climates *Earth Surf. Dyn.* **7** 345–60
- Meredith E P, Rust H W and Ulbrich U 2018 A classification algorithm for selective dynamical downscaling of precipitation extremes *Hydrol. Earth Syst. Sci.* **22** 4183–200
- Hazeleger W, Van den Hurk B J J M, Min E, Van Oldenborgh G J, Petersen A C, Stainforth D A, Vasileiadou E and Smith L A 2015 Tales of future weather *Nat. Clim. Change* **5** 107–13
- Chan S C, Kendon E J, Roberts N M, Fowler H J and Blenkinsop S 2016 The characteristics of summer sub-hourly rainfall over the southern uk in a high-resolution convective permitting model *Environ. Res. Lett.* **11** 094024
- Kendon E J, Blenkinsop S and Fowler H J 2018 When will we detect changes in short-duration precipitation extremes? *J. Clim.* **31** 2945–64
- Dunkerley D 2019 How does sub-hourly rainfall intermittency bias the climatology of hourly and daily rainfalls? Examples from arid and wet tropical Australia *Int. J. Climatol.* **39** 2412–21
- Burgueño A, Austin J, Vilar E and Puigcerver M 1987 Analysis of moderate and intense rainfall rates continuously recorded over half a century and influence on microwave communications planning and rain-rate data acquisition *IEEE Trans. Commun.* **35** 382–95
- Casas M C, Codina B, Redano A and Lorente J 2004 A methodology to classify extreme rainfall events in the western Mediterranean area *Theor. Appl. Climatol.* **77** 139–50
- Lebeaupin C, Ducrocq V and Giordani H 2006 Sensitivity of torrential rain events to the sea surface temperature based on

- high-resolution numerical forecasts *J. Geophys. Res.: Atmos.* **111** D12110
- [28] Cornes R C, van der Schrier G, van den Besselaar E J M and Jones P D 2018 An ensemble version of the E-OBS temperature and precipitation data sets *J. Geophys. Res.: Atmos.* **123** 9391–409
- [29] Lana X, Serra C, Casas-Castillo M C, Rodríguez-Solà R, Redaño A and Burgueño A 2018 Rainfall intensity patterns derived from the urban network of Barcelona (NE Spain) *Theor. Appl. Climatol.* **133** 385–403
- [30] Lana X, Casas-Castillo M C, Serra C, Raúl Rodríguez-Solà, Redaño A, Burgueño A and Martínez M D 2019 Return period curves for extreme 5-min rainfall amounts at the Barcelona urban network *Theor. Appl. Climatol.* **135** 1243–57
- [31] Rodríguez R, Navarro X, Casas M C and Redaño A 2013 Rainfall spatial organization and areal reduction factors in the metropolitan area of Barcelona (Spain) *Theor. Appl. Climatol.* **114** 1–8
- [32] Casas M C, Rodríguez R and Redaño A 2010 Analysis of extreme rainfall in Barcelona using a microscale rain gauge network *Meteorol. Appl.* **17** 117–23
- [33] Habib E, Krajewski W F and Kruger A 2001 Sampling errors of tipping-bucket rain gauge measurements *J. Hydrol. Eng.* **6** 159–66
- [34] Wang J, Fisher B L and Wolff D B 2008 Estimating rain rates from tipping-bucket rain gauge measurements *J. Atmos. Oceanic Technol.* **25** 43–56
- [35] Herrera S, Fernández J and Gutiérrez J M 2016 Update of the Spain02 gridded observational dataset for EURO-CORDEX evaluation: assessing the effect of the interpolation methodology *Int. J. Climatol.* **36** 900–8
- [36] Rockel B, Will A and Hense A 2008 The regional climate model COSMO-CLM (CCLM) *Meteorol. Z.* **17** 347–8
- [37] Dee D P *et al* 2011 The ERA-interim reanalysis: configuration and performance of the data assimilation system *Q. J. R. Meteor. Soc.* **137** 553–97
- [38] Kotlarski S *et al* 2014 Regional climate modeling on European scales: a joint standard evaluation of the EURO-CORDEX RCM ensemble *Geosci. Model. Dev.* **7** 1297–333
- [39] Jacob D *et al* 2014 EURO-CORDEX: new high-resolution climate change projections for European impact research *Reg. Environ. Change* **14** 563–78
- [40] Meredith E P and Ulbrich U 2018 BINGO EURO-CORDEX Evaluation (Hamburg: World Data Center for Climate (WDCC) at DKRZ) (http://cera-www.dkrz.de/WDCC/ui/Compact.jsp?acronym=DKRZ_LTA_961_ds00002)
- [41] Maraun D and Widmann M 2015 The representation of location by a regional climate model in complex terrain *Hydrol. Earth Syst. Sci.* **19** 3449–56
- [42] Coles S 2001 *An Introduction to Statistical Modeling of Extreme Values* (London: Springer)
- [43] Heffernan J E, Stephenson A G and Gilleland E 2018 *ismev: An Introduction to Statistical Modeling of Extreme Values*, 2018. R package version 1.42
- [44] Klingaman N P, Martin G M and Moise A 2017 ASoP (v1. 0): a set of methods for analyzing scales of precipitation in general circulation models *Geosci. Model Dev.* **10** 57–83
- [45] Utsumi N, Seto S, Kanae S, Maeda E E and Oki T 2011 Does higher surface temperature intensify extreme precipitation? *Geophys. Res. Lett.* **38** L16708
- [46] Siegmund J F, Siegmund N and Donner R V 2017 CoinCalc new R package for quantifying simultaneities of event series *Comput. Geosci.* **98** 64–72
- [47] Chan S C, Kendon E J, Fowler H J, Blenkinsop S, Ferro C A T and Stephenson D B 2013 Does increasing the spatial resolution of a regional climate model improve the simulated daily precipitation? *Clim. Dyn.* **41** 1475–95
- [48] Lenderink G and Van Meijgaard E 2008 Increase in hourly precipitation extremes beyond expectations from temperature changes *Nat. Geosci.* **1** 511
- [49] Dai A 2006 Precipitation characteristics in eighteen coupled climate models *J. Clim.* **19** 4605–30
- [50] Berg P, Wagner S, Kunstmann H and Schädler G 2013 High resolution regional climate model simulations for Germany: part I-validation *Clim. Dyn.* **40** 401–14
- [51] Volosciuk C, Maraun D, Semenov V A and Park W 2015 Extreme precipitation in an atmosphere general circulation model: impact of horizontal and vertical model resolutions *J. Clim.* **28** 1184–205
- [52] Zhang X, Zwiers F W, Li G, Wan H and Cannon A J 2017 Complexity in estimating past and future extreme short-duration rainfall *Nat. Geosci.* **10** 255
- [53] Prein A F, Rasmussen R M, Ikeda K, Liu C, Clark M P and Holland G J 2017 The future intensification of hourly precipitation extremes *Nat. Clim. Change* **7** 48
- [54] Drobinski P *et al* 2018 Scaling precipitation extremes with temperature in the Mediterranean: past climate assessment and projection in anthropogenic scenarios *Clim. Dyn.* **51** 1237–57
- [55] Boessenkool B, Bürger G and Heistermann M 2017 Effects of sample size on estimation of rainfall extremes at high temperatures *Nat. Hazards Earth Syst. Sci.* **17** 1623–9
- [56] Knist S, Goergen K and Simmer C 2018 Evaluation and projected changes of precipitation statistics in convection-permitting WRF climate simulations over Central Europe *Clim. Dyn.* (<https://doi.org/10.1007/s00382-018-4147-x>)
- [57] Tölle M H, Schefczyk L and Gutjahr O 2018 Scale dependency of regional climate modeling of current and future climate extremes in Germany *Theor. Appl. Climatol.* **134** 829–48
- [58] Broucke S V, Wouters H, Demuzere M and van Lipzig N P M 2019 The influence of convection-permitting regional climate modeling on future projections of extreme precipitation: dependency on topography and timescale *Clim. Dyn.* **52** 5303–24
- [59] NCL 2018 The NCAR Command Language (Version 6.5.0) [Software]. (2018) (Boulder, Colorado:UCAR/NCAR/CISL/TDD) (<https://doi.org/10.5065/D6WD3XH5>)
- [60] R Core Team 2018 *R: A Language and Environment for Statistical Computing* (Vienna, Austria: R Foundation for Statistical Computing)
- [61] Meredith E P, Ulbrich U and Rust H W 2019 BINGO Badalona 0.02 degree evaluation simulations (Hamburg: World Data Center for Climate (WDCC) at DKRZ) (http://cera-www.dkrz.de/WDCC/ui/Compact.jsp?acronym=DKRZ_LTA_961_ds00007)